2015 IEEE 54th Annual Conference on Decision and Control (CDC)
December 15-18, 2015. Osaka, Japan

Pseudo-Range Navigation with Clock Offset and Propagation Speed Estimation

Pedro Batista, Carlos Silvestre, and Paulo Oliveira

Abstract— **This paper presents a novel long baseline navigation solution based on pseudo-range measurements that does not require clock synchronization nor propagation speed profiling. In a one-way-travel-time setting, the offset between the clocks of the emitters and the clock of the receiver is assumed unknown, as well as the speed of propagation of the acoustic waves in the medium. The proposed solution, which resorts to state and output augmentation to achieve a system that is linear in the state, is shown to yield estimates that converge exponentially fast to zero for all initial conditions. The observability of the system is also carefully analyzed, the multi-rate nature of the measurements is taken into account, and simulation results evidence excellent performance.**

I. INTRODUCTION

Long baseline (LBL) acoustic positioning systems are widely used in underwater navigation, mostly in one of two alternative modes: i) in one-way-travel-time (OWTT) LBL configurations, the clocks are assumed synchronized, the speed of propagation of the acoustic waves is assumed available, and the time of signal emission is either predefined or encoded and sent through communication modems, see [1], [2], from which the distances between several known emitters and the receiver installed on-board the vehicle are computed; or ii) in two-way-travel-time (TWTT) LBL configurations, a transponder installed on-board the vehicle interrogates a set of known transponders that are fixed in the mission scenario and computes the distances between the vehicle and each of these transponders based on the round-trip travel time assuming that the speed of propagation of the acoustic signals is available. Clock synchronization at the beginning of each mission poses an additional and very heavy burden. Furthermore, clock drift is inevitable in long missions unless synchronization is performed periodically. On the other hand, the speed of propagation of the waves in the medium depends on several characteristics such as the salinity, pressure, and temperature and it is either measured or profiled, often prior to the experiments. If that is not the case, or even for small errors of the sound velocity profile, the range measurements can carry large errors, particularly when the distances become large, thus putting into question the entire navigation data. This paper proposes to address both issues, simultaneously, with a novel OWTT navigation filter that explicitly estimates both the clock offset and the speed of propagation of the acoustic waves in the medium.

Early references on underwater acoustic positioning systems can be found in [3] and [4], whereas work on LBL can be found in [5], [6], [7], and [8]. For interesting discussions and detailed surveys on underwater vehicle navigation techniques and challenges see [9] and [10].

Previous work by the authors includes [11], [12], and [13]. In the first, a perfect TWTT LBL setting is assumed, with known speed of propagation of the acoustic waves in the medium. That quantity is explictly estimated in the later, while the second work considers a OWTT LBL setting but explicitly estimates the clock offset between the emitters and the receiver. The main contribution of this paper is the design a novel navigation filter that unifies both concepts. In short, a OWTT navigation setting is assumed but the clock of the receiver installed on-board does not need to be synchronized with those of the emitters. Additionally, the speed of propagation of the acoustic waves in the medium is also unknown. A filtering solution is proposed, bringing together the concepts introduced in [12] and [13], that yields estimates of the inertial position, inertial ocean current, clock offset, and speed of propagation of the acoustic waves. This setting potentially reduces the required hardware and simplifies deployment, as the clock of the vehicle does not need to be synchronized and the speed of sound does not need to be profiled. The discrete-time nature of the pseudo-range measurements is taken into account, the observability of the system is carefully analyzed, and the errors of the estimates, provided by a Kalman filter, converge exponentially fast to zero for all initial conditions. Higher rate attitude and velocity measurements drive the system dynamics between pseudo-range measurement updates.

A. Notation

Throughout the paper the symbol $\mathbf{0}$ denotes a matrix of zeros and $\mathbf{I}$ an identity matrix, both of appropriate dimensions. A block diagonal matrix is represented by $\operatorname{diag}(\mathbf{A}_1, \ldots, \mathbf{A}_n)$. For $\mathbf{x} \in \mathbb{R}^3$ and $\mathbf{y} \in \mathbb{R}^3$, $\mathbf{x} \cdot \mathbf{y}$ and $\mathbf{x} \times \mathbf{y}$ represent the inner and cross products, respectively.

This work was supported by the Fundação para a Ciência e a Tecnologia (FCT) through ISR under LARSyS UID/EEA/50009/2013, and through IDMEC, under LAETA UID/EMS/50022/2013 contracts, by the University of Macau Project MYRG2015-00127-FST, and by the Macau Science and Technology Development Fund under Grant FDCT/065/2014/A.

The authors are with the Institute for Systems and Robotics, Laboratory of Robotics and Engineering Systems, Portugal. Pedro Batista is also with Instituto Superior Técnico, Universidade de Lisboa, Portugal. C. Silvestre is with the Department of Electrical and Computer Engineering of the Faculty of Science and Technology of the University of Macau, Macau, China, on leave from Instituto Superior Técnico, Universidade de Lisboa, Lisboa, Portugal. Paulo Oliveira is also with the Department of Mechanical Engineering, Instituto Superior Técnico, Universidade de Lisboa, Portugal.

Emails: {pbatista,pjcro}@isr.ist.utl.pt, csilvestre@umac.mo

For convenience, define also the transpose operator $(.)^T$, and notice that $\mathbf{x} \cdot \mathbf{y} = \mathbf{x}^T \mathbf{y}$, $\mathbf{x}, \mathbf{y} \in \mathbb{R}^3$.

II. Problem statement

Consider a scenario where a set of acoustic emitters are installed in an LBL configuration and an underwater vehicle, equipped with an acoustic receiver, operates. The emitters are fixed, their clocks are synchronized and their inertial positions are available to the vehicle. Periodically, the emitters send acoustic signals, which are received by the vehicle. Additionally, the vehicle is also equipped with a Doppler velocity log (DVL) and an attitude and heading reference system (AHRS). In a typical OWTT-LBL positioning system, the clocks of the emitters and the vehicle are synchronized, time tags are sent along the acoustic signals, and the speed of propagation of the waves is known, so that the vehicle can determine directly the distance to each emitter. Two key differences are considered in this paper: i) the speed of propagation of the waves is not known; and ii) the clock of the vehicle is not necessarily synchronized with those of the emitters. The problem addressed in this paper is that of designing a continuous-discrete filter, with globally exponentially stable error dynamics, to estimate the inertial position and velocity of the vehicle, as well as the offset between the emitting and receiving clocks and the speed of propagation of the acoustic waves in the medium.

A. System dynamics

Denote by $\{\mathcal{I}\}$ a local inertial coordinate frame and by $\{\mathcal{B}\}$ a coordinate frame attached to the vehicle, usually referred to as the body-fixed reference frame. The linear motion of the vehicle satisfies

$$\dot{\mathbf{p}}(t) = \mathbf{R}(t)\mathbf{v}(t), \tag{1}$$

where $\mathbf{p}(t) \in \mathbb{R}^3$ corresponds to its inertial position, $\mathbf{v}(t) \in \mathbb{R}^3$ is the velocity of the vehicle relative to $\{\mathcal{I}\}$, expressed in $\{\mathcal{B}\}$, and $\mathbf{R}(t)$ is the rotation matrix from $\{\mathcal{B}\}$ to $\{\mathcal{I}\}$.

The attitude of the vehicle, encoded by $\mathbf{R}(t)$, is provided by the AHRS, whereas the DVL measures, in the absence of bottom-lock, the velocity of the vehicle relative to the fluid, expressed in body-fixed coordinates. Denote by $\mathbf{v}_c(t) \in \mathbb{R}^3$ the velocity of the fluid, in inertial coordinates, and by $\mathbf{v}_r(t) \in \mathbb{R}^3$ the DVL reading, i.e., the velocity of the vehicle relative to the fluid, expressed in body-fixed coordinates. Then, the inertial velocity of the vehicle, expressed in body-fixed coordinates, satisfies

$$\mathbf{v}(t) = \mathbf{R}^T(t)\mathbf{v}_c(t) + \mathbf{v}_r(t). \tag{2}$$

Finally, denote by $\mathbf{s}_i \in \mathbb{R}^3$, $i = 1, \ldots, L$, the inertial positions of the acoustic emitters. Then, the pseudo-range measurements can be written as

$$r_i(k) = v_s(t_k) \|\mathbf{s}_i - \mathbf{p}(t_k)\| + b_c(t_k), \tag{3}$$

with $t_k := t_0 + kT$, $k \in \mathbb{N}$, where $T > 0$ is the sampling period, t_0 is the initial time, $b_c(t_k)$ is a bias term that accounts for the effect of the unknown offset of the clocks between the emitters and the receiver, and $v_s(t_k)$ is the term that accounts for the unknown speed of propagation of the acoustic waves in the medium. Notice that $v_s(t_k)$ is not the speed of propagation of the acoustic waves in the medium. Instead, it is an unknown dimensionless scaling factor that accounts for the difference between the actual unknown speed of propagation of the acoustic waves in the medium and the nominal speed that is assumed by the range sensor. Likewise, $b_c(t_k)$ is not the actual clock offset. Instead, it corresponds to the distance offset that results from the clock offset at the actual speed of propagation of the acoustic waves in the medium.

The following assumptions are considered in the paper.

Assumption 1: The pseudo-range measurements are positive, i.e., $r_i(k) > 0$ for all k and $i = 1, \ldots, L$.

Assumption 2: The inertial fluid velocity, the speed of propagation of the acoustic waves in the medium, and the offset of the clocks are constant, i.e.,

$$\begin{cases} \dot{\mathbf{v}}_c(t) = \mathbf{0} \\ \dot{v}_s(t) = 0 \\ \dot{b}_c(t) = 0 \end{cases}.$$

Combining (1)-(3) and considering Assumption 2 gives the nonlinear system with discrete outputs

$$\begin{cases} \dot{\mathbf{p}}(t) = \mathbf{v}_c(t) + \mathbf{R}(t)\mathbf{v}_r(t) \\ \dot{\mathbf{v}}_c(t) = \mathbf{0} \\ \dot{v}_s(t) = 0 \\ \dot{b}_c(t) = 0 \\ r_1(k) = v_s(t_k) \|\mathbf{s}_1 - \mathbf{p}(t_k)\| + b_c(t_k) \\ \vdots \\ r_L(k) = v_s(t_k) \|\mathbf{s}_L - \mathbf{p}(t_k)\| + b_c(t_k) \end{cases}. \tag{4}$$

The problem considered in this paper is the design of an estimator for (4) with exponentially stable error dynamics.

III. Filter design

The two main issues regarding LBL navigation that are addressed in this paper, namely i) dealing with unknown speeds of propagation of the acoustic waves in the medium; and ii) dealing with unknown clock offsets between the emitters and the receivers have been addressed in the past. In particular, the later was considered in [12], where a novel long baseline navigation solution was proposed considering that there is an unknown clock offset between the acoustic emitters and the receiver. In that work, discrete-time pseudo-range measurements were considered, the system dynamics were augmented with the pseudo-range differences and the LBL geometry was also encoded through an augmented output in such a way that the resulting system dynamics could be considered as linear. The former was considered in [13], where the state was redefined considering scaled position and linear velocity states, augmenting also the state with the pseudo-range measurements, and considering also an augmented output to encode the LBL geometry of the problem, in such a way that the resulting system, although nonlinear, could be treated resorting to linear systems theory. This paper addresses both issues simultaneously, considering discrete-time pseudo-range measurements, with unknown clock offset, which results in biased pseudo-range measurements, and unknown speed of propagation of the acoustic waves in the medium, which results in scaled pseudo-range measurements. This setting leads to a nonlinear problem, which is tackled resorting to different but complementary approaches that lead to a system that can be regarded as linear, even though it still is inherently nonlinear.

A. Discretization and system augmentation

The exact discrete-time system dynamics corresponding to (4) are given by

$$\begin{cases} \mathbf{p}(t_{k+1}) = \mathbf{p}(t_k) + T\mathbf{v}_c(t_k) + \int_{t_k}^{t_{k+1}} \mathbf{R}(\tau)\mathbf{v}_r(\tau)\,d\tau \\ \mathbf{v}_c(t_{k+1}) = \mathbf{v}_c(t_k) \\ v_s(t_{k+1}) = v_s(t_k) \\ b_c(t_{k+1}) = b_c(t_k) \\ r_1(k) = v_s(t_k)\|\mathbf{s}_1 - \mathbf{p}(t_k)\| + b_c(t_k) \\ \vdots \\ r_L(k) = v_s(t_k)\|\mathbf{s}_L - \mathbf{p}(t_k)\| + b_c(t_k) \end{cases}. \tag{5}$$

In a similar fashion to [12], but considering also the clock offset, define the discrete-time states

$$\begin{cases} \mathbf{x}_1(k) := v_s^2(t_k)\,\mathbf{p}(t_k) \\ \mathbf{x}_2(k) := v_s^2(t_k)\,\mathbf{v}_c(t_k) \\ x_3(k) := v_s^2(t_k) \\ x_4(k) = b_c(t_k) \end{cases}, \tag{6}$$

which correspond to a scaled inertial position of the vehicle, a scaled inertial current velocity, and factors that account for the speed of propagation of the acoustic signals in the medium and the clock offset. From (5) one may write

$$\begin{cases} \mathbf{x}_1(k+1) = \mathbf{x}_1(k) + T\mathbf{x}_2(k) + x_3(k)\,\mathbf{u}(k) \\ \mathbf{x}_2(k+1) = \mathbf{x}_2(k) \\ x_3(k+1) = x_3(k) \\ x_4(k+1) = x_4(k) \end{cases},$$

with $\mathbf{u}(k) := \int_{t_k}^{t_{k+1}} \mathbf{R}(\tau)\mathbf{v}_r(\tau)\,d\tau$.

Next, equations that encode the LBL structure of the problem are derived. To that purpose, rearrange (3) as

$$r_i(k) - b_c(t_k) = v_s(t_k)\|\mathbf{s}_i - \mathbf{p}(t_k)\|,\ i = 1, \ldots, L. \tag{7}$$

Using the state definition (6), taking the square of the left side of (7) and expanding yields

$$[r_i(k) - b_c(t_k)]^2 = r_i^2(k) + x_4^2(k) - 2r_i(k)\,x_4(k), \tag{8}$$

$i = 1, \ldots, L$. On the other hand, taking the square of both sides of (7), expanding the right side, and taking into consideration the state definition (6) gives

$$[r_i(k) - b_c(t_k)]^2 = x_3(k)\left(\|\mathbf{s}_i\|^2 + \|\mathbf{p}(t_k)\|^2\right) - 2\mathbf{s}_i \cdot \mathbf{x}_1(k), \tag{9}$$

$i = 1, \ldots, L$. Now, considering (8) and (9) for different pairs of emitters and taking the differences allows to conclude

$$2\frac{\mathbf{s}_i - \mathbf{s}_j}{r_i(k)+r_j(k)} \cdot \mathbf{x}_1(k) - \frac{\|\mathbf{s}_i\|^2 - \|\mathbf{s}_j\|^2}{r_i(k)+r_j(k)} x_3(k) \\ -2\frac{r_i(k)-r_j(k)}{r_i(k)+r_j(k)} x_4(k) + [r_i(k) - r_j(k)] = 0 \tag{10}$$

for all $i, j \in \{1, \ldots, L\}$, $i \neq j$. Notice that (10) effectively encodes the LBL structure of the problem. This derivation bears resemblance with those presented in [12], [13], and [14]. However, in [14], neither the clock offset nor the speed of propagation of the acoustic signals were considered; in [12] the clock offset is considered but not the speed of propagation of the acoustic signals; in [13] the speed of propagation of the acoustic signals is considered but not the clock offset.

As it is interesting in terms of filtering performance, the differences between the pseudo-ranges measurements are also included in the system state. Define these new states as

$$\begin{cases} x_5(k) = r_1(k) - r_2(k) \\ x_6(k) = r_1(k) - r_3(k) \\ \vdots \\ x_{4+C_2^L}(k) = r_{L-2}(k) - r_L(k) \\ x_{5+C_2^L}(k) = r_{L-1}(k) - r_L(k) \end{cases},$$

where C_2^L is the number of 2-combinations of L elements, i.e., $C_2^L = L(L-1)/2$. It is a matter of tedious but straightforward computation to show that the dynamics of the new states can be written as

$$\begin{aligned} r_i(k+1) - r_j(k+1) = &-2T\frac{\mathbf{s}_i - \mathbf{s}_j}{r_i(k+1)+r_j(k+1)} \cdot \mathbf{x}_2(k) \\ &-2\frac{(\mathbf{s}_i - \mathbf{s}_j)\cdot\mathbf{u}(k)}{r_i(k+1)+r_j(k+1)} x_3(k) \\ &+2\frac{[r_i(k+1)-r_i(k)]-[r_j(k+1)-r_j(k)]}{r_i(k+1)+r_j(k+1)} x_4(k) \\ &+\frac{r_i(k)+r_j(k)}{r_i(k+1)+r_j(k+1)}[r_i(k) - r_j(k)] \end{aligned}$$

for all $i, j \in \{1, \ldots, L\}$, $i \neq j$.

Define the augmented state vector as

$$\mathbf{x}(k) := \left[\, \mathbf{x}_1^T(k)\ \mathbf{x}_2^T(k)\ x_3(k)\ x_4(k)\ x_5(k)\ \ldots\ x_{4+C_2^L}(k) \,\right]^T,$$

$\mathbf{x}(k) \in \mathbb{R}^{3+3+2+C_2^L}$. Then, the discrete-time state equation can be written as

$$\mathbf{x}(k+1) = \mathbf{A}(k)\,\mathbf{x}(k),$$

where $\mathbf{A}(k) \in \mathbb{R}^{(8+C_2^L)\times(8+C_2^L)}$,

$$\mathbf{A}(k) = \left[\begin{array}{cccc|c} \mathbf{I} & T\mathbf{I} & \mathbf{0} & \mathbf{0} & \mathbf{0} \\ \mathbf{0} & \mathbf{I} & \mathbf{0} & \mathbf{0} & \mathbf{0} \\ \mathbf{0} & \mathbf{0} & 1 & 0 & \mathbf{0} \\ \mathbf{0} & \mathbf{0} & 0 & 1 & \mathbf{0} \\ \hline \mathbf{0} & \mathbf{A}_{52}(k) & \mathbf{A}_{53}(k) & \mathbf{A}_{54}(k) & \mathbf{A}_{55}(k) \end{array}\right],$$

with

$$\mathbf{A}_{52}(k) = -2T \begin{bmatrix} \frac{\mathbf{s}_1^T - \mathbf{s}_2^T}{r_1(k+1)+r_2(k+1)} \\ \frac{\mathbf{s}_1^T - \mathbf{s}_3^T}{r_1(k+1)+r_3(k+1)} \\ \vdots \\ \frac{\mathbf{s}_{L-2}^T - \mathbf{s}_L^T}{r_{L-2}(k+1)+r_L(k+1)} \\ \frac{\mathbf{s}_{L-1}^T - \mathbf{s}_L^T}{r_{L-1}(k+1)+r_L(k+1)} \end{bmatrix} \in \mathbb{R}^{C_2^L \times 3},$$

$$\mathbf{A}_{53}(k) = -2 \begin{bmatrix} \frac{(\mathbf{s}_1 - \mathbf{s}_2)\cdot\mathbf{u}(k)}{r_1(k+1)+r_2(k+1)} \\ \frac{(\mathbf{s}_1 - \mathbf{s}_3)\cdot\mathbf{u}(k)}{r_1(k+1)+r_3(k+1)} \\ \vdots \\ \frac{(\mathbf{s}_{L-2} - \mathbf{s}_L)\cdot\mathbf{u}(k)}{r_{L-2}(k+1)+r_L(k+1)} \\ \frac{(\mathbf{s}_{L-1} - \mathbf{s}_L)\cdot\mathbf{u}(k)}{r_{L-1}(k+1)+r_L(k+1)} \end{bmatrix},$$

$$\mathbf{A}_{54}(k) = 2 \begin{bmatrix} \frac{[r_1(k+1)-r_1(k)]-[r_2(k+1)-r_2(k)]}{r_1(k+1)+r_2(k+1)} \\ \frac{[r_1(k+1)-r_1(k)]-[r_3(k+1)-r_3(k)]}{r_1(k+1)+r_3(k+1)} \\ \vdots \\ \frac{[r_{L-2}(k+1)-r_{L-2}(k)]-[r_L(k+1)-r_L(k)]}{r_{L-2}(k+1)+r_L(k+1)} \\ \frac{[r_{L-1}(k+1)-r_{L-1}(k)]-[r_L(k+1)-r_L(k)]}{r_{L-1}(k+1)+r_L(k+1)} \end{bmatrix},$$

and

$$\mathbf{A}_{55}(k) = \mathbf{diag}\left(\frac{r_1(k)+r_2(k)}{r_1(k+1)+r_2(k+1)}, \frac{r_1(k)+r_3(k)}{r_1(k+1)+r_3(k+1)}, \ldots, \frac{r_{L-2}(k)+r_L(k)}{r_{L-2}(k+1)+r_L(k+1)}, \frac{r_{L-1}(k)+r_L(k)}{r_{L-1}(k+1)+r_L(k+1)}\right).$$

In order to the define the augmented system, discard the original nonlinear output, consider (10) and notice that the states $x_5(k), \ldots, x_{4+C_2^L}(k)$ are available from the pseudo-range measurements, which gives in compact form

$$\begin{cases} \mathbf{x}(k+1) = \mathbf{A}(k)\,\mathbf{x}(k) \\ \mathbf{y}(k+1) = \mathbf{C}(k+1)\mathbf{x}(k+1) \end{cases}, \tag{11}$$

with $\mathbf{C}(k) \in \mathbb{R}^{2C_2^L \times \left(8+C_2^L\right)}$,

$$\mathbf{C}(k) = \begin{bmatrix} \mathbf{0} & \mathbf{0} & \mathbf{0} & \mathbf{0} & \mathbf{I} \\ \mathbf{C}_{21}(k) & \mathbf{0} & \mathbf{C}_{23}(k) & \mathbf{C}_{24}(k) & \mathbf{I} \end{bmatrix},$$

$$\mathbf{C}_{21}(k) = 2\begin{bmatrix} \frac{\mathbf{s}_1^T - \mathbf{s}_2^T}{r_1(k)+r_2(k)} \\ \frac{\mathbf{s}_1^T - \mathbf{s}_3^T}{r_1(k)+r_3(k)} \\ \vdots \\ \frac{\mathbf{s}_{L-2}^T - \mathbf{s}_L^T}{r_{L-2}(k)+r_L(k)} \\ \frac{\mathbf{s}_{L-1}^T - \mathbf{s}_L^T}{r_{L-1}(k)+r_L(k)} \end{bmatrix},$$

$$\mathbf{C}_{23}(k) = -\begin{bmatrix} \frac{\|\mathbf{s}_1\|^2 - \|\mathbf{s}_2\|^2}{r_1(k)+r_2(k)} \\ \frac{\|\mathbf{s}_1\|^2 - \|\mathbf{s}_3\|^2}{r_1(k)+r_3(k)} \\ \vdots \\ \frac{\|\mathbf{s}_{L-2}\|^2 - \|\mathbf{s}_L\|^2}{r_{L-2}(k)+r_L(k)} \\ \frac{\|\mathbf{s}_{L-1}\|^2 - \|\mathbf{s}_L\|^2}{r_{L-1}(k+r_L(k)} \end{bmatrix},$$

and

$$\mathbf{C}_{24}(k) = -2\begin{bmatrix} \frac{r_1(k)-r_2(k)}{r_1(k)+r_2(k)} \\ \frac{r_1(k)-r_3(k)}{r_1(k)+r_3(k)} \\ \vdots \\ \frac{r_{L-2}(k)-r_L(k)}{r_{L-2}(k)+r_L(k)} \\ \frac{r_{L-1}(k)-r_L(k)}{r_{L-1}(k+r_L(k)} \end{bmatrix}.$$

Notice that the system (11) is well defined under Assumption 1. Moreover, the system matrix $\mathbf{A}(k)$ is invertible for all time.

B. Observability analysis

The discrete time-varying system (11) can be regarded as linear in the state for observer design purposes, even though the system matrices $\mathbf{A}(k)$ and $\mathbf{C}(k)$ depend on the pseudo-range measurements, as well as on the input $\mathbf{u}(k)$. This is possible because for observer (or filter) design purposes, both the input and the pseudo-ranges are available and, hence, they can be simply considered as functions of time. The following result addresses the observability of the discrete-time system (11).

Theorem 1: Define, for $k_i \geq k_0$,

$$\mathbf{L}(k_i) := \begin{bmatrix} \mathbf{L}_1(k_i) & \mathbf{L}_2(k_i) & \mathbf{L}_3(k_i) \end{bmatrix} \in \mathbb{R}^{C_2^L \times 5},$$

with

$$\mathbf{L}_1(k_i) := 2\begin{bmatrix} (\mathbf{s}_1 - \mathbf{s}_2)^T \\ (\mathbf{s}_1 - \mathbf{s}_3)^T \\ \vdots \\ (\mathbf{s}_{L-2} - \mathbf{s}_L)^T \\ (\mathbf{s}_{L-1} - \mathbf{s}_L)^T \end{bmatrix} \in \mathbb{R}^{C_2^L \times 3},$$

$$\mathbf{L}_2(k_i) := -\begin{bmatrix} \|\mathbf{s}_1\|^2 - \|\mathbf{s}_2\|^2 \\ \|\mathbf{s}_1\|^2 - \|\mathbf{s}_3\|^2 \\ \vdots \\ \|\mathbf{s}_{L-2}\|^2 - \|\mathbf{s}_L\|^2 \\ \|\mathbf{s}_{L-1}\|^2 - \|\mathbf{s}_L\|^2 \end{bmatrix} \in \mathbb{R}^{C_2^L},$$

and

$$\mathbf{L}_3(k_i) := -2\begin{bmatrix} r_1(k_i) - r_2(k_i) \\ r_1(k_i) - r_3(k_i) \\ \vdots \\ r_{L-2}(k_i) - r_L(k_i) \\ r_{L-1}(k_i) - r_L(k_i) \end{bmatrix} \in \mathbb{R}^{C_2^L}.$$

Suppose that the configuration of the LBL acoustic positioning system is such that $\mathbf{L}(k_i)$ is full rank, i.e.,

$$\mathrm{rank}(\mathbf{L}(\mathrm{k_i})) = 5, \tag{12}$$

Then, the discrete-time system (11) is observable on $[k_i, k_i+2]$, in the sense that the initial state $\mathbf{x}(k_i)$ is uniquely determined by the input $\{\mathbf{u}(k) : k = k_i, k_i+1\}$ and the output $\{\mathbf{y}(k) : k = k_i, k_i+1\}$.

Proof: The proof reduces to show that the observability matrix $\boldsymbol{\mathcal{O}}(k_i, k_i+2)$ associated with the pair $(\mathbf{A}(k), \mathbf{C}(k))$ on $[k_i, k_i+2]$, $k_i \geq k_0$, has rank equal to the number of states of the system. It is omitted due to the lack of space. ∎

As in [12] or [13], there is nothing in the augmented system imposing certain constraints, which were discarded so that the system could be regarded as linear. In particular, the original nonlinear outputs, as a function of the original states, were ignored. Moreover, there is nothing in the augmented system (11) imposing the nonlinear constraints of the new augmented states with respect to the original system states. As such, one must further establish the equivalence between both systems, (5) and (11), which is the topic of the following theorem.

Theorem 2: Suppose that (12) holds for some $k_i \geq k_0$. Then:

i) the nonlinear system (5) is observable on the interval $[k_i, k_i+2]$ in the sense that the initial state $\mathbf{x}(k_i)$ is uniquely determined by the input $\{\mathbf{u}(k) : k = k_i, k_i+1\}$ and the output $\{r_1(k), \ldots, r_L(k) : k = k_i, k_i+1\}$; and

ii) the initial condition of the augmented system (11) matches that of (5) on the interval $[k_i, k_i+2]$, i.e.,

$$\begin{cases} \mathbf{x}_1(k_i) = v_s^2(t_{k_i})\,\mathbf{p}(t_{k_i}) \\ \mathbf{x}_2(k_i) = v_s^2(t_{k_i})\,\mathbf{v}_c(t_{k_i}) \\ x_3(k_i) = v_s^2(t_{k_i}) \\ x_4(k_i) = b_c(t_{k_i}) \\ x_5(k_i) = v_s(t_{k_i})\left[\|\mathbf{s}_1 - \mathbf{p}(t_{k_i})\| - \|\mathbf{s}_2 - \mathbf{p}(t_{k_i})\|\right] \\ x_6(k_i) = v_s(t_{k_i})\left[\|\mathbf{s}_1 - \mathbf{p}(t_{k_i})\| - \|\mathbf{s}_3 - \mathbf{p}(t_{k_i})\|\right] \\ \vdots \\ x_{3+C_2^L}(k_i) = v_s(t_{k_i})\left[\|\mathbf{s}_{L-2} - \mathbf{p}(t_{k_i})\| - \|\mathbf{s}_L - \mathbf{p}(t_{k_i})\|\right] \\ x_{4+C_2^L}(k_i) = v_s(t_{k_i})\left[\|\mathbf{s}_{L-1} - \mathbf{p}(t_{k_i})\| - \|\mathbf{s}_L - \mathbf{p}(t_{k_i})\|\right] \end{cases}.$$

Proof: The second part of the theorem follows by comparison of the outputs of both systems as a function of the initial states. It is omitted due to the lack of space. Then, notice that, using Theorem 1, the initial condition of (11) is uniquely determined. As, in addition, the two initial conditions match, it follows that the initial condition of (5) is also uniquely determined. ∎

C. Estimation solution

1) Augmented system: An observer (or filter) for the augmented system (11) readily gives estimates of $v_s^2(t_k)\,\mathbf{p}(t_k)$, $v_s^2(t_k)\,\mathbf{v}_c(t_k)$, $v_s^2(t_k)$, and $b_c(t_k)$. As it was seen the system dynamics (11) can be regarded as linear for observer (of filter) design purposes. A Kalman filter is an obvious choice, yielding globally exponentially stable error dynamics if the system is shown to be uniformly completely observable. Here, only observability was shown due to space limitations but the proof of uniform complete observability, while tedious, follows similar steps considering uniform bounds in time.

2) Estimation between range measurements: Any observer (or filter) for the discrete-time augmented system (11) only provides estimates when pseudo-range measurements are available. However, the DVL and the AHRS usually provide data at higher rates. Hence it is possible to obtain estimates of the scaled position, scaled velocity, and the two factors that account for the speed to propagation of the acoustic waves and the clock offset, at a higher rates, using open-loop propagation between pseudo-range measurements.

3) Estimates of $\mathbf{p}(t)$, $\mathbf{v}_c(t)$, and $v_s(t)$: The estimates provided by an observer (or filter) for the augmented system (11) do not correspond exactly to what one aims to estimate, as the inertial position and ocean current velocity are scaled and the factor that accounts for the speed of propagation of the acoustic waves in the medium is squared. Nevertheless, estimates for $\mathbf{p}(t_k)$, $\mathbf{v}_c(t_k)$, and $v_s(t)$ can be recovered, under some mild assumptions. As this has been detailed in [13], only the main results are shown.

Assumption 3: The speed of propagation of the acoustic waves in the medium satisfies

$$V_m \leq v_s(t) \leq V_M,$$

with $V_m, V_M > 0$. Moreover, the inertial position of the vehicle and the ocean current velocity are norm-bounded.

Considering estimates $\hat{x}_3(t)$ with globally exponentially stable error dynamics, the estimate of the speed of propagation of the acoustic waves in the medium can be obtained from

$$\hat{v}_s(t) = \begin{cases} V_m, & \hat{x}_3(t) < V_m^2 \\ \sqrt{\hat{x}_3(t)}, & V_m^2 \leq \hat{x}_3(t) \leq V_M^2 \\ V_M, & \hat{x}_3(t) > V_M^2 \end{cases},$$

whose error converges exponentially fast to zero for all initial conditions under Assumption 3. Estimates for the position and ocean current velocity then follow from

$$\begin{cases} \hat{\mathbf{p}}(t) = \frac{\hat{\mathbf{x}}_1(t)}{\hat{v}_s^2(t)} \\ \hat{\mathbf{v}}_c(t) = \frac{\hat{\mathbf{x}}_2(t)}{\hat{v}_s^2(t)} \end{cases},$$

and it is possible to show that, under Assumption 3, these also converge exponentially fast to zero for all initial conditions.

IV. Simulation results

This section presents briefly some simulation results in order to illustrate the excellent performance achieved by the proposed solution. The initial position of the vehicle is $\mathbf{p}(0) = [0\,0\,10]^T$ m, while the ocean current velocity was set to $\mathbf{v}_c(t) = [0.1\; -0.2\; 0]^T$ m/s. The trajectory that was described by the vehicle is shown in Fig. 1, which lasts one hour. In the simulations presented herein, the

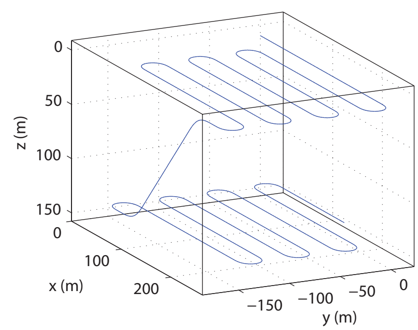

Fig. 1. Trajectory described by the vehicle

LBL configuration is composed of 5 acoustic beacons and their inertial positions are $\mathbf{s}_1 = \begin{bmatrix} 0 & 0 & 0 \end{bmatrix}^T$ (m), $\mathbf{s}_2 = \begin{bmatrix} 0 & 0 & 500 \end{bmatrix}$ (m), $\mathbf{s}_3 = \begin{bmatrix} 500 & 0 & 500 \end{bmatrix}$ (m), $\mathbf{s}_4 = \begin{bmatrix} 1000 & 0 & 500 \end{bmatrix}$ (m), and $\mathbf{s}_5 = \begin{bmatrix} 0 & 750 & 500 \end{bmatrix}$ (m), so that the rank condition (12) is satisfied. The scale factor that accounts for the unknown speed of propagation of the acoustic waves was set to $v_s = 1.05$, while the term that accounts for the clocks' offset was set to $b_c = 50$ m.

Sensor noise was considered for all sensors. In particular, the LBL range measurements and the DVL relative velocity readings were assumed to be corrupted by additive uncorrelated zero-mean white Gaussian noise, with standard deviations of 1 m and 0.01 m/s, respectively. The attitude, provided by the AHRS and parameterized by roll, pitch, and yaw Euler angles, was also assumed to be corrupted by zero-mean, additive white Gaussian noise, with standard deviation of $0.03°$ for the roll and pitch and $0.3°$ for the yaw. The sampling period for the range measurements was set to $T = 10$ s, while the remaining sensors were sampled at 5 Hz. The discrete-time input $\mathbf{u}(k)$, corresponding to a definite integral, was approximated using the trapezoid rule, while the open-loop solution of the position and ocean current velocity estimates, between range measurements, was computed using the Euler method. In fact, as it also corresponds to a definite integral, it is equivalent to the application of the trapezoid rule.

To tune the Kalman filter, the state disturbance covariance matrix was chosen as

$$\operatorname{diag}\left(10/0.2 \times 0.01^2\mathbf{I},\, 0.001^2\mathbf{I},\, 0.01^2,\, 0.01^2,\, 10^{-4}\mathbf{I}\right)$$

and the output noise covariance matrix was set to $\operatorname{diag}\left(2\mathbf{I},\, 0.2\mathbf{I}\right)$. The initial condition for the scaled position was set with a large initial error, $\hat{\mathbf{x}}_1(0) = [200\,200\,200]^T\,(\mathrm{m})$, while the initial estimates of both the ocean current velocity and term that accounts for the offset between the clocks were set to zero. The initial estimate of the factor that accounts for the unknown speed of propagation was set with an error of 10%. The initial estimates of the pseudo-range differences were set according to the first measurement set that was obtained.

The convergence of the position and velocity errors is depicted in Figs. 2 and 3. The discrete-time updates are visible in these figures, as well as the open-loop propagation intervals. As it is possible to observe, the error converges

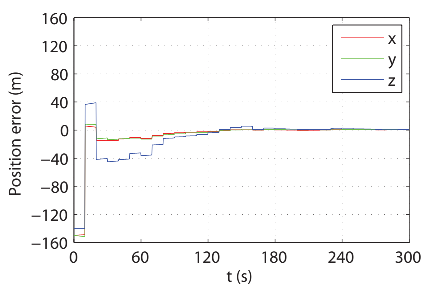

Fig. 2. Initial convergence of the position error

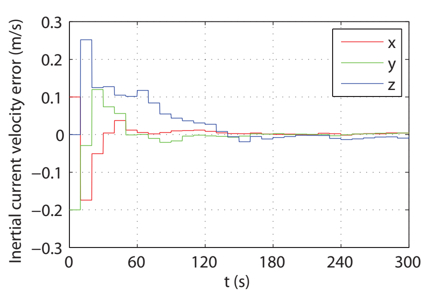

Fig. 3. Initial convergence of the ocean current velocity error

very fast to a neighborhood of zero (due to the presence of sensor noise, otherwise it would converge to zero). The convergence of the factors that account for the speed of propagation and the acoustic waves and the clock offset errors are now shown due to the lack of space but similar behaviors occur. The detailed evolutions, in steady-state, of the errors of the position and velocity are not shown either. However, the most noticeable feature is that the position and velocity errors remain, most of the time, below $1\,\mathrm{m}$ and $0.005\,\mathrm{m/s}$, respectively. In steady-state, the position error does not surpass $2\,\mathrm{m}$ and the inertial current velocity error does not surpass $0.015\,\mathrm{m/s}$, which are excellent results considering the sensor suite noise, low update times, and the demanding framework, which includes estimation of the clock offset and speed of propagation of the acoustic signals.

V. Conclusions

This paper proposed a novel solution for OWTT LBL navigation with explicit estimation of the clock offset between the receiver and the emitters and the speed of propagation of the acoustic waves in the medium. The design is constructive, with the derivation of a novel augmented system that can be regarded as linear in the state for observer design purposes. Its observability was analyzed and a Kalman filter provides the estimation solution. The final estimates feature exponential convergence to the true values for all initial conditions and the multi-rate characteristics of the sensors were taken into consideration. Finally, simulation results evidence excellent performance.

References

[1] R. Eustice, L. Whitcomb, H. Singh, and M. Grund, "Experimental Results in Synchronous-Clock One-Way-Travel-Time Acoustic Navigation for Autonomous Underwater Vehicles," in *Proceedings of the 2007 Int. Conference on Robotics and Automation*, Rome, Italy, Apr. 2007, pp. 4257–4264.

[2] S. Webster, R. Eustice, H. Singh, and L. Whitcomb, "Advances in single-beacon one-way-travel-time acoustic navigation for underwater vehicles," *The International Journal of Robotic Research*, vol. 31, no. 8, pp. 935–950, Jul. 2012.

[3] M. Hunt, W. Marquet, D. Moller, K. Peal, W. Smith, and R. Spindel, "An acoustic navigation system," Woods Hole Oceanographic Institution, Tech. Rep. Technical Report 74-6, Dec. 1974.

[4] P. Milne, *Underwater Acoustic Positioning Systems*. Gulf Publishing Co, 1983.

[5] L. Techy, K. Morgansen, and C. Woolsey, "Long-baseline acoustic localization of the Seaglider underwater glider," in *Proceedings of the 2011 American Control Conference*, San Francisco, USA, Jun.-Jul. 2011, pp. 3990–3995.

[6] L. Whitcomb, D. Yoerger, and H. Singh, "Combined Doppler/LBL Based Navigation of Underwater Vehicles," in *Proceedings of the 11th International Symposium on Unmanned Untethered Submersible Technology*, Durham, New Hampshire, USA, Aug. 1999, pp. 1–7.

[7] J. Vaganay, J. Bellingham, and J. Leonard, "Comparison of fix computation and filtering for autonomous acoustic navigation," *Int. J. of Systems Science*, vol. 29, no. 10, pp. 1111–1122, Oct. 1998.

[8] J. Kinsey and L. Whitcomb, "Preliminary field experience with the DVLNAV integrated navigation system for oceanographic submersibles," *Control Engineering Practice*, vol. 12, no. 12, pp. 1541–1548, Dec. 2004.

[9] J. Kinsey, R. Eustice, and L. Whitcomb, "A Survey of Underwater Vehicle Navigation: Recent Advances and New Challenges," in *Proceedings of the 7th IFAC Conf. on Manoeuvring and Control of Marine Craft*, Lisboa, Portugal, Sep. 2006.

[10] H.-P. Tan, R. Diamant, W. Seah, and M. Waldmeyer, "A survey of techniques and challenges in underwater localization," *Ocean Engineering*, vol. 38, no. 14-15, pp. 1663–1676, Oct. 2011.

[11] P. Batista, C. Silvestre, and P. Oliveira, "Sensor-based Long Baseline Navigation: observability analysis and filter design," *Asian Journal of Control*, vol. 16, no. 4, pp. 974–994, Jul. 2014.

[12] P. Batista, "Long baseline navigation with clock offset estimation and discrete-time measurements," *Control Engineering Practice*, vol. 35, pp. 43–53, Feb. 2015.

[13] P. Batista, "GES Long Baseline Navigation with Unknown Sound Velocity and Discrete-time Range Measurements," *IEEE Transactions on Control Systems Technology*, vol. 23, no. 1, pp. 219–230, Jan. 2015.

[14] J. Caffery, "A new approach to the geometry of TOA location," in *Proceedings of the IEEE VTS Fall VTC2000 52nd Vehicular Technology Conference*, vol. 4, Boston, USA, Sep. 2000, pp. 1943–1949.